ISSN: 0067-2904

Antibacterial Activity of Green-Synthesized Zinc Oxide Nanoparticles from *Ganoderma lucidum* Mushroom Extract Against Multidrug-Resistant Bacteria: An in Vitro Study

Hasan Jamal Kareem*, Alaa Mohsin Al-Araji
Department of Biology, College of Science, University of Baghdad, Baghdad, Iraq

Received: 2/10/2024 Accepted: 27/2/2025 Published: 28/2 /2026

Abstract

The green synthesis of nanoparticles is regarded as an eco-friendly, cost-effectiveness, and simple methodology. Using green synthesis techniques for nanoparticles may enhance the characteristics of these nanomaterials through reduced dimensions and specific shapes achieved. *Ganoderma lucidum* mushroom has numerous bioactive compounds, such as proteins, polysaccharides, and secondary metabolites, which can act as reducing and stabilizing agents in nanoparticles synthesis. The antibacterial activity of zinc oxide nanoparticles (ZnO-NPs) has received considerable interest due to their ability to interact with bacterial surfaces and penetrate the bacterial core, hence revealing unique bactericidal mechanisms. This study explores the green synthesis of ZnO-NPs using *G. lucidu*m extract as a reducing agent. The fruiting bodies powder was extracted with hot water in a shaking water bath at 75 °C with 40 rpm for 2 hours, then filtered to obtain *G. lucidum* aqueous extract. The nanoparticles, synthesized by reacting zinc chloride salt with the extract, were characterized using UV, FTIR, AFM, EDX, and FESEM. The antibacterial activity of ZnO-NPs was evaluated using the agar well diffusion method. The characterization techniques confirmed the successful biosynthesis of ZnO-NPs, revealing a diameter of 44.62 nm, and the particles formed were spherical, hexagonal, and triangular. Antibacterial activity was tested against four MDR bacterial strains (*Staphylococcus aureus*, *Enterococcus faecalis*, *Pseudomonas aeruginosa*, and *Escherichia coli*), showing significant efficacy. The highest inhibition zone (23.333 mm) was observed for *S. aureus* at a ZnO-NPs concentration of 100 mg/ml. This finding has significance in revealing an eco-friendly antibacterial agent as an alternative to conventional antibiotics.

Keywords: *Ganoderma lucidum*, Zinc oxide nanoparticles, Green synthesis, MDR

النشاط المضاد للبكتريا لجسيمات أوكسيد الزنك النانوية المصنَّعة بالطريقة الخضراء من مستخلص فطر *Ganoderma lucidum* ضد البكتريا المتعددة المقاومة للمضادات الحيوية: دراسة مختبرية

حسن جمال كريم*, علاء محسن الاعرجي
قسم علوم الحياة, كلية العلوم, جامعة بغداد, بغداد, العراق

الخلاصة

يعتبر التخليق الأخضر للجسيمات النانوية صديقًا للبيئة وفعالًا من حيث التكلفة والمنهجية البسيطة. ان استخدام تقنيات التخليق الأخضر للجسيمات النانوية يؤدي إلى تعزيز خصائص هذه المواد النانوية من خلال

*Email: hasan.jamal2302@sc.uobaghdad.edu.iq

تعزيز صغر الاحجام والشكل المحدد الذي يتم تحقيقه. يحتوي فطر *Ganoderma lucidum* على العديد من المركبات النشطة بيولوجيًا مثل البروتينات والسكريات المتعددة ومركبات الايض الثانوية، والتي يمكن أن تعمل كعوامل اختزال وتثبيت في تخليق الجسيمات النانوية. لقد حظي النشاط المضاد للبكتريا لجسيمات أوكسيد الزنك النانوية باهتمام كبير بسبب قدرتها على التفاعل مع سطح البكتريا واختراق مركز البكتريا، وبالتالي الكشف عن آليات فريدة من نوعها لقتل الميكروبات. تهدف هذه الدراسة الى التخليق الأخضر لجسيمات أوكسيد الزنك النانوية باستخدام مستخلص فطر *Ganoderma lucidum* كعامل مختزل. تم استخلاص مسحوق الأجسام الثمرية بالماء الساخن في حمام مائي هزاز بدرجة حرارة 75 درجة مئوية بسرعة 40 دورة في الدقيقة لمدة ساعتين، ثم ترشيح المزيج للحصول على مستخلص *Ganoderma lucidum* المائي. تم تشخيص الجسيمات النانوية المصنعة حيويا عن طريق تفاعل ملح كلوريد الزنك مع المستخلص، بأستخدام مطياف الأشعة فوق البنفسجية ومطياف الاشعة تحت الحمراء ومجهر القوة الذرية ومطياف تشتت الطاقة بالاشعة السينية والمجهر الالكتروني الماسح الباعث. تم تقييم النشاط المضاد للبكتريا لجسيمات أوكسيد الزنك النانوية من خلال طريقة الانتشار بالأغار. أكدت تقنيات التشخيص المستخدمة نجاح عملية التخليق الحيوي لجسيمات أوكسيد الزنك النانوية، والتي كانت بقطر 44.62 نانومتر وكانت الجسيمات المتكونة كروية وسداسية ومثلثة. تم اختبار النشاط المضاد للبكتريا ضد أربع سلالات بكتيرية متعددة المقاومة للمضادات الحيوية وهي بكتريا المكورات العنقودية الذهبية وبكتريا المكورات المعوية البرازية وبكتريا الزائفة الزنجارية وبكتريا الاشريكية القولونية. حيث اظهرت الدقائق النانوية نشاطا مضادا للبكتريا بشكل كبير. لوحظت ان أعلى منطقة تثبيط كانت بقطر 23.333 مليميتر للمكورات العنقودية الذهبية عند تركيز من جسيمات اوكسيد الزنك النانوية بمقدار 100 مجم / مل. هذه الدراسة لها أهمية لأكتشاف عامل مضاد للبكتريا صديق للبيئة كبديل للمضادات الحيوية التقليدية.

1. Introduction

Nanotechnology includes the generation and management of nano-scale information inside a confined region of materials, devices, and measurements. Nano data is utilized in the form of constituent particles, known as nanoparticles (NPs), which are composed of atoms and molecules with a range from 1 to 100 nm dimensions. It is extensively employed to develop more effective methodologies in the fields of technology, energy conservation, studies in science, medicine, and many other fields. NPs are generated by different approaches, including biological, chemical and physical methods. These methods are classified into bottom-up and top-down methods [1]. Among these methods, biological or green synthesis is a type of bottom-up approach, that utilizes natural and environmentally friendly materials as reducing agents. Some green materials are also being used as end-capping agents and dispersants at the same time [2]. The green synthesis of nanoparticles is considered eco-friendly, cost-effectiveness, and simple methodology. However, using green synthesis techniques for nanoparticles may enhance the characteristics of these nanomaterials by means of the reduced dimensions and specific shape achieved, as well as the unique qualities of the biological substrates employed [3].

Among these nanoparticles, zinc oxide nanoparticles (ZnO-NPs) belong to a class of metal oxide nanomaterials that possess distinctive physical and chemical properties. They are inorganic chemical substances that have extensive applications in daily life. ZnO-NPs are the most utilized metal oxide nanoparticles due to their unique optical and chemical properties, which can be readily adjusted by modifying their morphology, wide bandgap, and high excitation binding energy thereby enabling ZnO-NPs to be a potent photocatalytic and photo-oxidizing moiety against chemical and biological species [4]. They exhibit reduced toxicity to the human body and provide biocompatibility, as the Zn ion (Zn^{2+}), a soluble form of ZnO, is a trace element present in the human physiological system. ZnO has demonstrated biodegradability in both bulk form and as nanoparticles [5].

One of the most important medicinal mushrooms is *Ganoderma lucidum* (*G. lucidum*), which was discovered over two thousand years ago and is used in traditional medicine. It has a broad spectrum of pharmaceutical and biological characteristics, it has been used for thousands of years as a health promotion and offering effective defence to the entire body [6]. *G. lucidum* are classified within the Phylum Basidiomycota, Class Agaricomycetes, Order: Polyporales, and Family Ganodermataceae. This mushroom has gained recognition as a significant medicinal mushroom due to its abundance of highly bioactive secondary metabolites. The biologically active compounds obtained from this mushroom consist of terpenoids, phenols, steroids, and nucleotides, in addition to glycoproteins and polysaccharides [7]. The bioactive compounds of this mushroom can act as reducing and stabilizing agents in nanoparticle synthesis. These compounds can enhance the morphology, size, and optical properties of the resulting ZnO-NPs [8].

Antibiotic resistance is the inability of antibiotics to kill or suppress microbial development, resulting in bacteria developing resistance to effective antibiotics. Key factors contributing to the evolution of antimicrobial resistance include the over use of antibiotics and inappropriate therapeutic prescriptions [9]. The growing number of microbial infections, along with antibiotic resistance, has been identified as a significant public health issue, encouraging the discovery of new treatments through the use of nanotechnology. Nanotechnology provides excellent solutions across several applications, with metallic nanoparticles recognized for their significant antibacterial efficacy against human infections [10]. Hence, the antibacterial activity of ZnO-NPs has received significant interest due to their ability to interact with bacterial surfaces and penetrate the bacterial core where they enter the cell, demonstrating unique bactericidal mechanisms [11]. ZnO-NPs synthesized using *G. lucidum* mushroom have additional potential for biomedical applications utilizing the medicinal advantages of this mushroom. The ZnO-NPs provide enhanced antibacterial and antimicrobial properties due to the inherent antibacterial nature of zinc [12].

The aims of this study are to estimate the green or biological synthesis of zinc oxide nanoparticles from the aqueous extract of *G. lucidum* mushroom, characterize these nanoparticles by several techniques, and evaluate the antibacterial activity of ZnO-NPs synthesized from *G. lucidum* aqueous extract.

2. Materials and Methods

2.1 Mushroom materials

Iraqi *G. lucidum* fruiting bodies were used in this study and obtained from National Centre of Organic Farming, Ministry of Agriculture, Baghdad, Iraq. For this study, thirty fruit bodies were collected in February 2024. These fruit bodies were dried at 45 °C for two days using a laboratory drier. The dried fruiting bodies were pulverized into powder by a laboratory grinder (Model FW100, Brand Carlssoon Technologies, Malaysia) [13].

2.2 Preparation of G. lucidum aqueous extract

Fruiting bodies powder was extracted with hot water (1:20, w/v) in a shaking water bath (Memmert, Germany) at 75 °C with 40 rpm for 2 h. The suspension was filtered using gauze and filter paper (Whatman no. 1). The aqueous extract was kept at 4 °C until use [14].

2.3 Collection of pathogenic bacteria

The pathogenic bacteria were collected from two hospitals located in Baghdad City. The hospitals are Al-Imam Ali General Hospital and Ghazy Al-Hariri Hospital for Surgical Specialties. 227 specimens were obtained from different sites of the bodies, including urine, ear swabs, sputum, faeces, wounds, and throat swabs from various ages of both genders. These bacteria were incubated at 37 ˚C for 24 hours and identified [15]. The pathogenic

bacteria were identified according to the morphological characteristics in the selective media of the developing bacteria in away colonies, such as textures, colony shape, colour, transparency, colonial boundaries, and growth intensity. In addition to morphological characteristics, the microscopic examination was applied by taking swabs from the growing bacterial colonies on slides and staining them with a dye to identify Gram-negative and Gram-positive bacteria. Plates that did not show growth after 24 hours were considered to be negative samples [16].

2.4 Antibiotic susceptibility test

The clinical bacterial isolates were tested for antibiotic susceptibility according to the guideline of CLSI, 2024. This guideline was applied to classify the bacteria as either sensitive (S), intermediate (I), or resistant (R) to the recommended antibiotics. This experiment was carried out through the disc diffusion method according to Bauer and Kirby's method in a basic procedure: two to four colonies were collected from bacterial isolates, then were suspended in 5 ml normal saline and calibrated the turbidity of bacterial suspension with McFarland standard 0.5 (1.5 x 10^8 cfu/ml). The bacterial suspensions were spread according to the Lawn Culture Method using sterile cotton swabs onto the surface of Muller Hinton Agar (MHA). The inoculated plates were left for 20 minutes to absorb the moisture. Following that, the discs of the recommended antibiotics were put on the surface of the inoculated plates and incubated at 37°C for 18 to 24 hours. After that, the inhibition zone diameter in millimeters was measured around each antibiotic disc, representing the bacterial susceptibility for each antibiotic [17].

2.5 VITEK-2 compact system

The four MDR bacterial isolates used in this study were identified, and the species were approved using the Vitek-2 compact system with several biochemical tests [18].

2.6 Synthesis of zinc oxide nanoparticles

The synthesis of ZnO-NPs was achieved by utilizing anhydrous zinc chloride salt (purchased from Alfa Chemika, India) as a precursor for Nano zinc synthesis. Zinc chloride was used with the aqueous extraction of *G. lucidum* at a ratio (1:10 w/v), then the suspensions were placed in a shaker at 150 rpm for 24 hours in dark conditions. The next day, the suspensions were placed in a centrifuge at 4830 x g for 15 minutes, the supernatants were eliminated, and the precipitates were collected then washed firstly with 10 ml of absolute ethanol and re-centrifuged, then washed with 10 ml of deionized distilled water and also centrifuged for 4830 x g for 15 minutes. The resulting precipitates were collected and located in an oven at 40 °C overnight. Subsequently, the precipitates were collected and placed in a test tube and kept in a dark condition for further use, including characterization and antibacterial applications [19].

2.7 Characterization of ZnO-NPs

According to Alden and Yaaqoob [20], several techniques were applied to investigate the green-produced ZnO-NPs powder, including:

2.7.1 Ultraviolet-Visible spectroscopy

The samples were measured by UV spectrophotometer type (UV-9200. Biotech Engineering Management CO. LTD. UK) to identify the optical absorption spectra of ZnO-NPs and *G. lucidum* aqueous extract [21].

2.7.2 Fourier transform infrared (FTIR)

The aqueous extract, zinc chloride salt, zinc oxide nanoparticles, and zinc chloride with the aqueous extract together were measured by FTIR-8400 (Shimadzu, Japan) to identify the differences in the structures of biomolecules by detecting the differences in the functional groups [22].

2.7.3 Atomic force microscopy (AFM)

The particle size and the three-dimensional visualization of ZnO-NPs were analysed using atomic force microscopy (Core-AFM 2023 model, manufactured by Nanosurf AG, Switzerland) [22].

2.7.4 Energy dispersive X-ray spectroscopy (EDX)

The three-dimensional elemental distribution and the percentage of atomic and weights of elements were analysed using EDX spectroscopy (Quattro S-2022, Thermo Fisher Scientific, Czech Republic) [21].

2.7.5 Field emission scanning electron microscope (FESEM)

FESEM is an approach that generates pictures of ZnO-NPs by directing an electron beam across its surface. This offered high-resolution, three-dimensional photographs of micron- and nanometer-sized particles. For this purpose, the size and shape of the green synthesized ZnO-NPs were analysed using Quattro S –STEM/SEM, Thermo Fisher Scientific, Czech Republic [23].

2.8 Antibacterial activity of ZnO-NPs

Five concentrations from nanoparticles were utilized to evaluate the antibacterial efficacy of ZnO-NPs: 6.25, 12.5, 25, 50, and 100 mg/ml. To ensure even dispersion of ZnO-NPs in deionized distilled water, an ultrasonication technique and vigorous shaking (using a vortex) were applied. The dispersion and stability of the sample were characterized visually. This experiment was carried out through the agar well diffusion method in a basic procedure: two to four colonies were collected from bacterial isolates and then were suspended in 5 ml normal saline (in plain tubes 10 ml), and calibrating the turbidity of the suspension with McFarland standard 0.5 (1.5×10^8 cfu/ml). The bacterial suspensions were spread according to the Lawn Culture Method by using sterile cotton swabs onto the surface of MHA media by turning the plates three times to distribute the bacteria evenly across the surface of the agar. The inoculated plates were left for 20 minutes to absorb the moisture. A well with 5 mm diameter was punched using a sterile cork borer, and then 60 µL from the mentioned concentrations was introduced into each well (each plate had five wells with five concentrations). The plates have been incubated at 37°C for 24 hours. After that, the inhibition zone diameter in millimeters was measured, representing the antibacterial effect of each concentration; each treatment has consisted of three replicates [24].

2.9 Statistical analysis

The statistical analysis was performed using the SPSS-25 program for data analysis according to the two-way analysis of variance (Tow –Way ANOVA). A complete randomized design (CRD) was established with three replicates per treatment. The means were separated using the Least Significant Differences test (LSD) and a P value of ≤ 0.05.

3. Results and Discussions

3.1 Collection of pathogenic bacteria

Four bacterial isolates were selected and used in this study that exhibited multi-drug resistance (MDR). These pathogenic bacteria were *Enterococcus faecalis*, *Staphylococcus aureus*, *Escherichia coli,* and *Pseudomonas aeruginosa.*

3.2 VITEK-2 compact system

The VITEK2 compact system identified the species of bacteria which were mentioned above; all bacteria had a 99% probability (Table 1).

Table 1: Identification information of VITEK-2 for the MDR-selected bacteria

Selected organism	Probability	Bionumber	Analysis time (hours)
Enterococcus faecalis	99%	116012761753471	3.12
Staphylococcus aureus	99%	010402062763031	3.83
Escherichia coli	99%	0405610454426611	3.38
Pseudomonas aeruginosa	99%	6222649203427140	16.8

3.3 Antibiotic susceptibility test

Out of 135 positive bacterial samples, four isolates were selected which were MDR. In other words, these four isolates were resistant to almost all antibiotics that were tested except a few antibiotics that were sensitive (Table 2).

Table 2: The result of antibiotic susceptibility testing for the selected bacteria (R: resistance, S: sensitive, I: intermediate).

Antibiotic	*E. coli*	*P. aeruginosa*	*S. aureus*	*E. faecalis*
Ampicillin	R	R	R	S
Azithromycin			R	R
Gentamycin	R	R	R	R
Vancomycin			S	S
Ciprofloxacin	R	R	R	R
Levofloxacin	R	R	S	S
Erythromycin	R			R
Tetracycline	R	R		R
Ceftazidime	R	R	R	R
Cefepime	R	R		
Trimethoprim	R		R	
Imipenem	S	S		
Ceftriaxone	R	R	S	R
Amikacin	S	S	R	R
Meropenem	S	R	R	

3.4 Synthesis of zinc oxide nanoparticles

The ZnO-NPs were synthesized utilizing the aqueous extract of *G. lucidum* mushroom due to their reducing and stabilizing agents. The synthesis of ZnO-NPs was verified through optical examination. The insertion of zinc chloride into the aqueous extract modified the color to yellow, suggesting the synthesis of ZnO-NPs. Following centrifugation and drying by oven, a brownish-white powder developed (Figure 1). The change in color indicates the

synthesis of the nanomaterial because the biological extracts contain variable secondary metabolites, which act as reducing agents [25]. This observation agreed with the findings of Abdullah*, et al.* [26].

Figure 1: Zinc oxide nanoparticles, which were green synthesized from the aqueous extract of *Ganoderma lucidum* mushroom

The biosynthesis of ZnO-NPs is an uncomplicated procedure wherein a zinc salt, such as zinc nitrate or zinc chloride, is introduced to a pre-prepared biological extract, resulting in the preparation of ZnO powder. The bio extracts containing secondary metabolites have the ability to reduce and capping of Zn(II) ions in salt solutions. Subsequently, the oxidation process can yield stable and uniformly dispersed ZnO-NPs [27].

Several studies have shown the efficacy of *G. lucidum* aqueous extract. Previous reports found that this extract contained not only polysaccharides but also *G. lucidum* triterpenoids, such as Ganoderma acid, Ganoderma aldehyde and Ganoderma ergosterol. In addition to that, the aqueous extract of this mushroom contains several bioactive phytochemicals such as nucleosides, alkaloids, coumarin, ergosterols, ganoderic acids, lactones, mannitol, organic germanium, triterpenoids, unsaturated fatty acids [28]. The bioactive compounds of this mushroom can act as reducing and stabilizing agents in nanoparticles synthesis [29].

3.5 Characterization of ZnO-NPs

3.5.1 Ultraviolet-Visible spectroscopy

The absorption peaks of the green synthesized ZnO-NPs and *G. lucidum* the aqueous extract, are shown in Figure 2. Each of the samples demonstrates significant UV absorption, with absorption peaks ranging from 287 to 303 nm. After additional diluting by deionized distilled water of the ZnO sample, the absorption peak was at 303 nm. This result corresponds to biosynthesized ZnO-NPs direct band emission. On the other hand, the absorption peak of the aqueous extract was at 289 nm. This result agreed with the study of Alden and Yaaqoob [20], which showed that ZnO-NPs exhibited a UV absorption at around 287 nm.

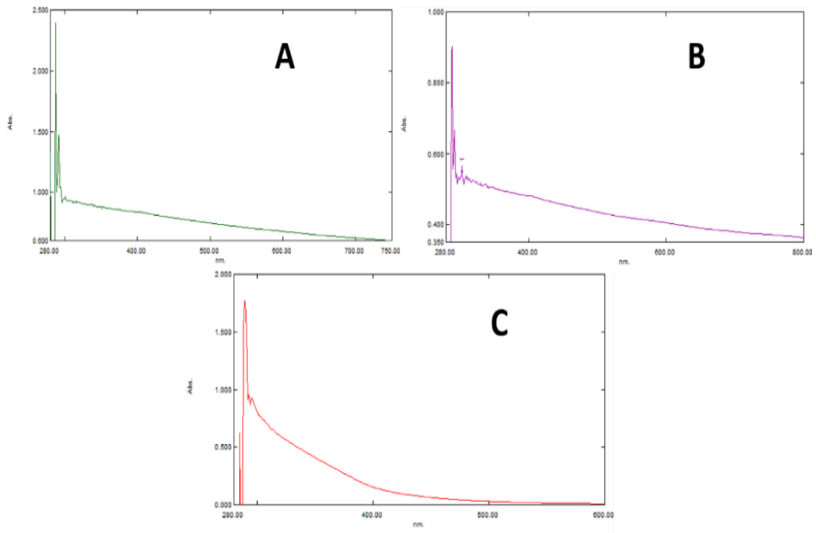

Figure 2: UV visible spectroscopy of ZnO-NPs and the *G. lucidum* aqueous extract, (A): diluted sample of ZnO-NPs, (B): very diluted sample of ZnO-NPs, (C): the aqueous extract.

3.5.2 Fourier transform infrared (FTIR)

Zinc oxide nanoparticles produced by green methods were examined using FTIR spectroscopy at wave numbers between 4000 cm^{-1} and 500 cm^{-1} to identify the phytochemicals responsible for stabilizing and capping the nanoparticles. Figure 3 displays the FTIR spectra of ZnO-NPs, *G. lucidum* aqueous extract, zinc chloride anhydrous salt, and zinc chloride with aqueous extract together. The high peaks of ZnO-NPs situated at 3440.77 and 3425.34 cm^{-1} indicated the existence of -OH groups. Other peaks were denoted for ZnO-NPs at 2921.96, 2368.42, 1645.17, 1515.94, 1110.92, 673.11, and 595.96. The ZnO-NPs stretching was at 424.31 cm^{-1}. The peaks of ZnO-NPs indicated the existence of O-H, C-H, and C-N stretching vibrations associated with aromatic and aliphatic amino groups. The FTIR of the aqueous extract has a highly intense peak at 2362.64 cm^{-1}, which can be related to C=N stretch. The N-H bond Amine I groups are also observed at 1645.17 cm^{-1}. For zinc chloride salt, the FTIR result was 3560.35, 3542.99, 2360.71, 1620.09, and peaks between 1402.15 and 432.03 cm^{-1}.

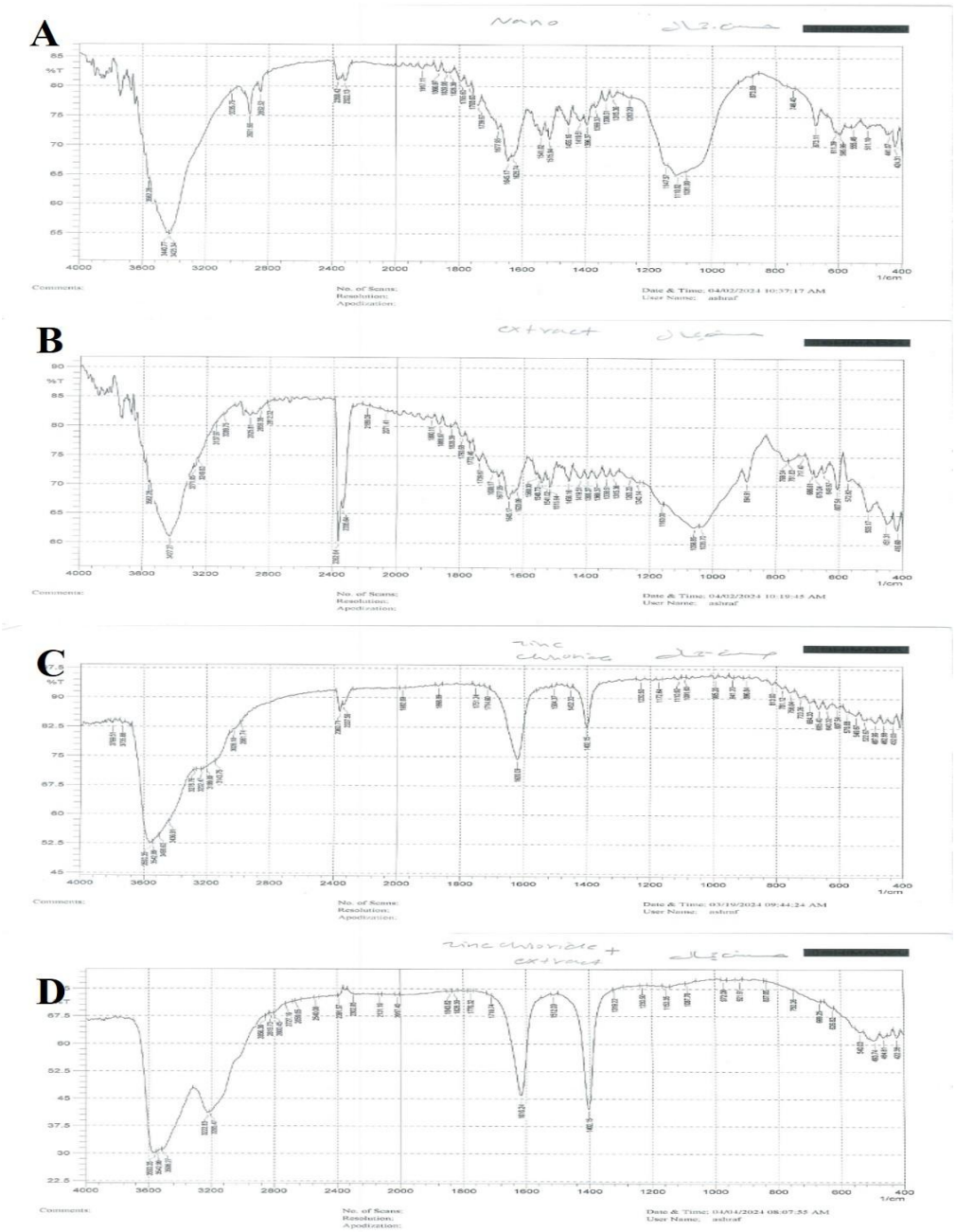

Figure 3: FTIR results: (A): ZnO-NPs. (B): Aqueous extract. (C): Zinc chloride salt. (D): Zinc chloride with aqueous extract together.

This result agreed with the study of Sanmugam*, et al.* [30] which produced a ZnO nanoparticles with chitosan, showing O-H stretching at around 3500 cm^{-1} and 1630 cm^{-1}, respectively. Additionally, the N-H deformation vibrations are seen at 1636 and 1562 cm^{-1}. The Zn-O stretch appears at around 424 cm^{-1}.

3.5.3 Atomic force microscopy (AFM)

AFM was used to analyze the shape and size of ZnO-NPs from two- and three-dimensional views. Figure 4 shows the 2D and 3D AFM images for ZnO-NPs. The 3D image of AFM showed a homogenous dispersion of ZnO-NPs with no visible agglomeration. The average diameter of ZnO-NPs was 44.62 nm, as shown in Figure 5.

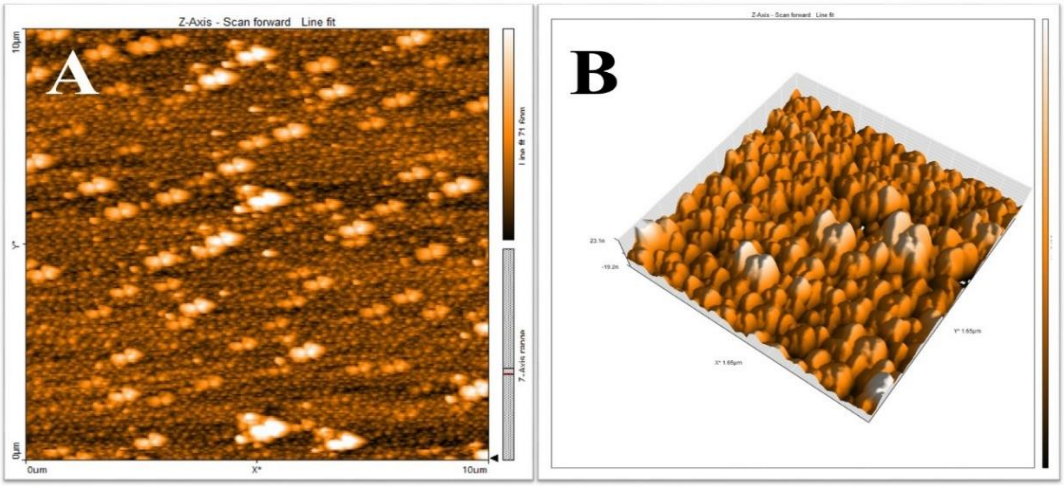

Figure 4: Atomic force analysis of the microscopic surface morphology of ZnO-NPs. (A): Two-dimensional view. (B): Three-dimensional view.

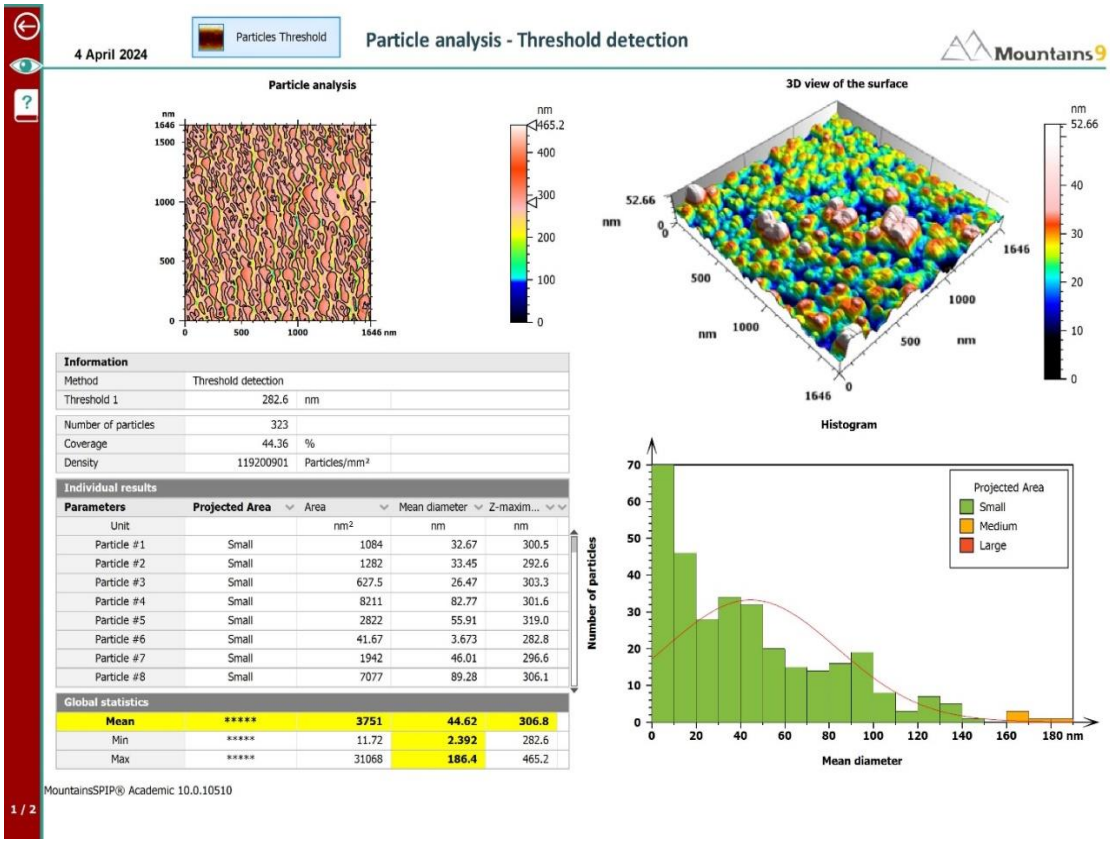

Figure 5: Average grain size of ZnO-NPs

3.5.4 Energy dispersive X-ray spectroscopy (EDX)

The examination of the elements of ZnO-NPs was conducted using EDX spectroscopy. The result in Table 3 shows a weight percentage of 22% for the Zn element and 45.9% for O. The EDX analysis of ZnO-NPs indicates the presence of zinc and oxygen as components present. The typical strong signal peaks at 1 and 8.5 keV for zinc and strong peak at 0.5 keV for oxygen are displayed by zinc oxide nanoparticles (Figure 6).

This result agreed with Agarwal, *et al.* [31], demonstrating that Zn exhibits peaks at about 1 keV, 8.6 keV, and 9.5 keV. On the other hand, O peak at around 0.5 Kev.

Table 3: The percentage of atomic and weight of elements in EDX analysis

Elements	Atomic %	Weight %
C	3.2	12.2
N	8.2	6.6
O	49.8	45.9
Zn	31.8	22.0
Al	0.8	1.2
Si	0.7	1.1
P	1.9	3.4
S	0.7	1.4
Cl	1.4	2.8
Ca	1.5	3.4

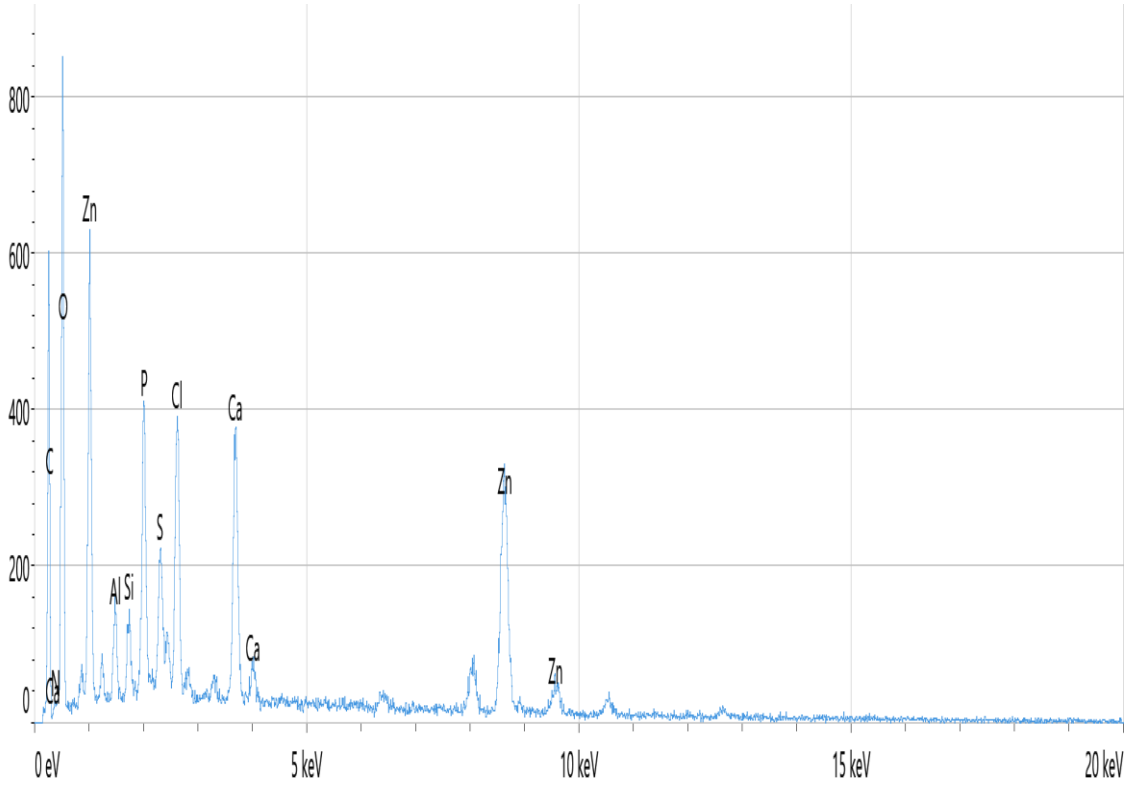

Figure 6: EDX image of the green synthesized ZnO-NPs

3.5.5 Field emission scanning electron microscope (FESEM)

The result of FESEM indicated that the particles formed were spherical, hexagonal, and triangular, as shown in Figure 7. FESEM analysis revealed that the particle size ranges from 43.24 to 64.16 nm. This finding significantly supports that *G. lucidum* aqueous extract could serve as a capping and reducing agent in synthesizing ZnO-NPs.

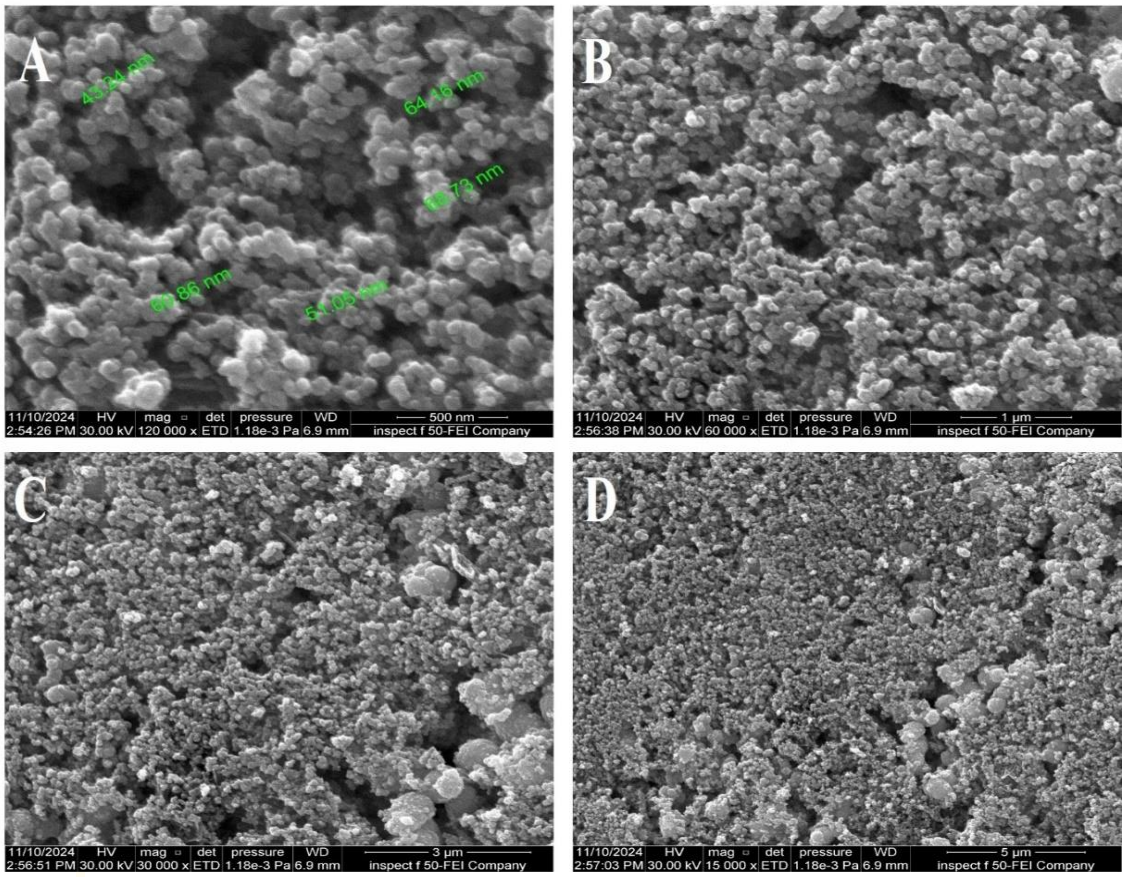

Figure 7: FESEM images at different magnification of the biosynthesized ZnO nanoparticles, (A): x120000. (B): x60000. (C): x30000. (D): x15000

3.6. Antibacterial activity of ZnO-NPs

The efficacy of ZnO-NPs against MDR bacterial isolates was evaluated depending on the zone of inhibition in comparison to the positive control (Ceftriaxone antibiotic) and negative control (deionized distilled water), which exhibited no inhibitory effect on bacteria in comparison to ZnO-NPs. The antibacterial effect of ZnO-NPs was studied against MDR G-ve bacteria (*P. aeruginosa* and *E. coli*) and G+ve bacteria (*S. aureus* and *E. faecalis*). The agar well diffusion method was applied to determine each bacterium's minimum inhibitory concentration (MIC) of ZnO-NPs.

Zinc oxide nanoparticles exhibited significant antibacterial activity against all tested MDR bacteria. For *S. aureus*, *P. aeruginosa,* and *E. coli*, the lower inhibition zone mean value was reported with a concentration of 6.25 mg/ml, and the higher inhibition zone mean value was recorded with a concentration of 100 mg/ml. Nevertheless, the lower inhibition zone mean value for *E. faecalis* was reported with a concentration of 50 mg/ml, and the higher inhibition zone was recorded with a 100 mg/ml concentration. Conversely, the positive control (Ceftriaxone antibiotic) exhibited no inhibition zone on all tested bacteria except for *S. aureus* which revealed a 10 mm zone of inhibition. The negative control (deionized distilled water) showed no inhibition zone on all tested bacteria. There are no significant differences between the antibiotic control and deionized distilled water (except for *S. aureus* treatment). The maximum inhibition zone was for *S. aureus* at a concentration of 100 mg/ml, which exhibited 23.333 mm. while the minimum inhibition was zero at 6.25, 12.5, and 25 mg/ml for *E. faecalis*. Moreover, the inhibition zone of ZnO-NPs significantly improved at increased concentrations on all tested bacteria, as shown in Table 4 and Figure 8.

Table 4: The inhibition zone (millimeter) of MDR bacterial isolates by using zinc oxide nanoparticles of *Ganoderma lucidum* aqueous extract at (6.25, 12.5, 25, 50, and 100 mg/ml) concentrations on Muller Hinton Agar during 24 hours of incubation at 37˚C (each treatment consisted of three replicates).

Concentrations / Bacteria	Inhibition zone (mm)							
	6.25 mg/ml	12.5 mg/ml	25 mg/ml	50 mg/ml	100 mg/ml	Ceftriaxone	Control	Mean
E. coli	5.667	7.667	10.333	15.667	18.333	0.000	0.000	8.238
P. aeruginosa	6.333	8.667	9.333	13.333	16.667	0.000	0.000	7.762
S. aureus	9.333	12.333	15.333	20.000	23.333	10.000	0.000	12.905
E. faecalis	0.000	0.000	0.000	9.667	15.000	0.000	0.000	3.524
Mean	5.333	7.167	8.750	14.667	18.333	2.500	0.000	
L S D	$P \leq 0.05$							
Between Concentrations	0.421**							
Between bacteria	0.557**							
Between interactions	1.1145**							

The inhibition zone of bacteria by NPs is identified by multiple theories regarding the properties of bacterial inhibition, such as the properties of nanoparticles involving their dependence on size, stability, and concentration introduced into the growth medium. This interaction duration increases due to the surface-to-volume ratio of NPs increasing by one million [32].

There are three primary mechanisms of antibacterial activity of ZnO-NPs: firstly, stimulate the generation of Reactive Oxygen Species (ROS), including superoxide anion (O^2), hydrogen peroxide (H_2O_2), and hydroxide (OH^-). The toxicity of these species involves the destruction of cellular components such as lipids, DNA, and proteins in bacteria. Secondly, the release of zinc ions from ZnO-NPs to the medium with bacteria, the releasing of Zn^{+2} significantly inhibits the active transport and disrupts amino acid metabolism and enzyme systems. Finally, it disrupts the plasma membrane, causing membrane dysfunction, resulting in their internalization into the bacteria [33].

Modern studies indicated that ZnO-NPs have antimicrobial properties by degrading the cell membranes and stimulating oxidative stress, which is very different from the antibacterial mechanisms of conventional antibiotics. ZnO-NPs enhanced the photocatalytic efficiency, improved biological compatibility, and greater selectivity. Furthermore, it exhibits heat resistance and stability. Moreover, ZnO-NPs exhibit important antimicrobial properties due to their small dimensions, activating diverse bactericidal mechanisms upon entry into bacterial cells. These mechanisms encompass the invasion of the bacterial surface or core, the stimulation of ROS, the release of Zn(II) ions, and even the absorption of zinc oxide by cells [34].

This result is in agreement with Verma*, et al.* [35], who examined the antibacterial effect of ZnO-NPs against collections of Gram-positive and Gram-negative bacteria. Their study showed that the highest antibacterial effect was noticed with a reduction in size and improvement in oxygen on the surface of ZnO-NPs. These nanoparticles exhibited damage in the bacterial plasma membrane by hydrophobic interactions and hydrogen bonding with amino acid groups in the proteins of the plasma membrane, following the destruction or breakdown of the membrane, completed by nanoparticle absorption and the beginning of oxidative stress.

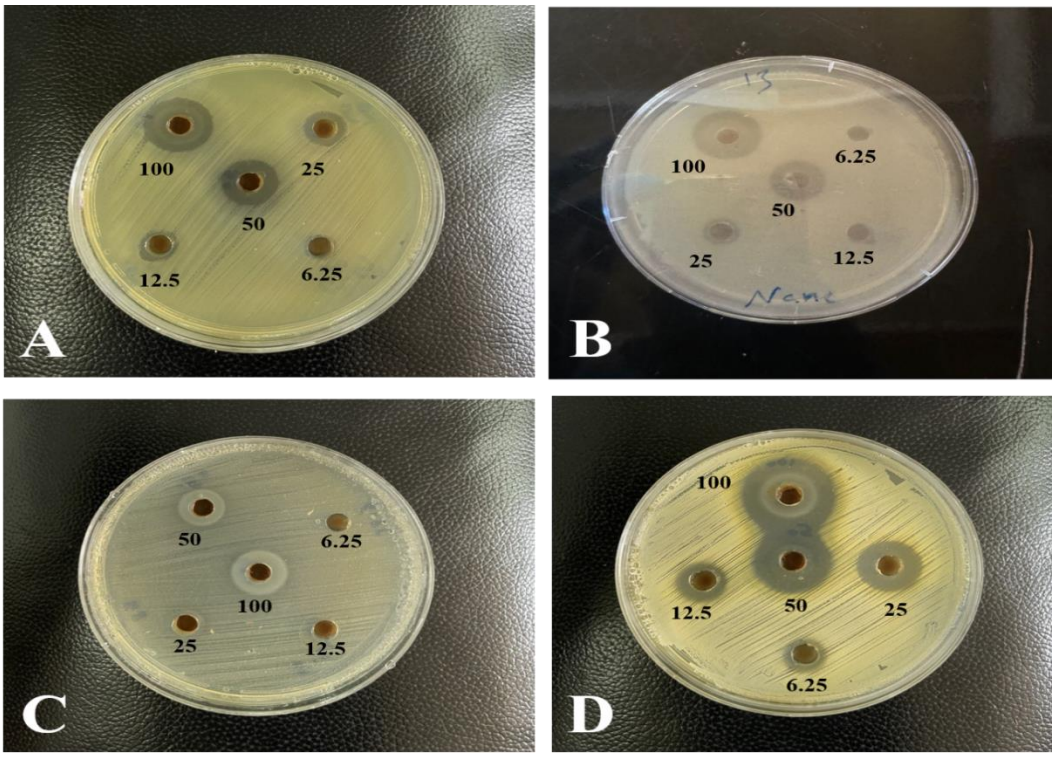

Figure 8: Antibacterial activity of zinc oxide nanoparticles on bacteria: (A): *P. aeruginosa*. (B): *E. coli*. (C): *E. faecalis.* (D): *S. aureus.*

4. Conclusion

This study provided an accurate guideline for the green synthesis of ZnO-NPs from the aqueous extract of *G. lucidum* mushroom. Several techniques were applied to characterize the green synthesized ZnO-NPs; these techniques approved the green synthesis of ZnO-NPs. The antibacterial activity of ZnO-NPs was evaluated against four MDR bacteria, which demonstrated resistance to several antibiotics. Hence, ZnO-NPs exhibited significant antibacterial activity against the MDR bacteria with different degrees. This study recommends employing the green synthesized ZnO-NPs for multiple biological applications.

5. Acknowledgements

We would like to thank Assistant Professor Dr. Laith Ahmed Yaaqoob in the Department of Biotechnology, College of Science, University of Baghdad. Also, special thanks to the National Centre of Organic Farming, Iraqi Ministry of Agriculture, for the help to successfully complete this study.

6. Ethical clearance

This study was ethically approved according to the reference number CSEC/1024/0065 by the ethical committee of the College of Science, University of Baghdad.

7. Conflict of interest

The authors declare that they have no conflicts of interest.

References

[1] N. Joudeh and D. Linke, "Nanoparticle classification, physicochemical properties, characterization, and applications: a comprehensive review for biologists," *Journal of Nanobiotechnology,* vol. 20, no. 1, p. 262, 2022.

[2] R. A. Banjara, A. Kumar, R. Aneshwari, M. L. Satnami, and S. Sinha, "A comparative analysis of chemical vs green synthesis of nanoparticles and their various applications," *Environmental Nanotechnology, Monitoring & Management,* p. 100988, 2024.

[3] I. Ijaz, E. Gilani, A. Nazir, and A. Bukhari, "Detail review on chemical, physical and green synthesis, classification, characterizations and applications of nanoparticles," *Green Chemistry Letters and Reviews,* vol. 13, no. 3, pp. 223-245, 2020.

[4] E. Y. Shaba, J. O. Jacob, J. O. Tijani, and M. A. T. Suleiman, "A critical review of synthesis parameters affecting the properties of zinc oxide nanoparticle and its application in wastewater treatment," *Applied Water Science,* vol. 11, no. 2, p. 48, 2021.

[5] A. K. Mandal, S. Katuwal, F. Tettey, A. Gupta, S. Bhattarai, S. Jaisi, D. P. Bhandari, A. K. Shah, N. Bhattarai, and N. Parajuli, "Current research on zinc oxide nanoparticles: synthesis, characterization, and biomedical applications," *Nanomaterials,* vol. 12, no. 17, p. 3066, 2022.

[6] D. Cor Andrejc, Z. Knez, and M. Knez Marevci, "Antioxidant, antibacterial, antitumor, antifungal, antiviral, anti-inflammatory, and nevro-protective activity of Ganoderma lucidum: An overview," *Frontiers in Pharmacology,* vol. 13, pp. 934-982, 2022.

[7] Z. Lin and B. Yang, *Ganoderma and Health Biology, Chemistry and Industry. Advances in Experimental Medicine and Biology*, 2019.

[8] A. Can and K. Kızılbey, "Green Synthesis of ZnO Nanoparticles via Ganoderma Lucidum Extract: Structural and Functional Analysis in Polymer Composites," *Gels,* vol. 10, no. 9, p. 576, 2024.

[9] D. K. Al-Fahad, J. A. Alpofead, M. A. Chawsheen, A. A. Al-Naqshbandi, and A. T. Abas, "Surveillance of Antimicrobial Resistance in Iraq," *Aro- The Scientific Journal of Koya University,* vol. 12, no. 2, pp. 179-193, 2024.

[10] F. Fatima, S. Siddiqui, and W. A. Khan, "Nanoparticles as novel emerging therapeutic antibacterial agents in the antibiotics resistant era," *Biological Trace Element Research,* vol. 199, no. 7, pp. 2552-2564, 2021.

[11] I. Kim, K. Viswanathan, G. Kasi, S. Thanakkasaranee, K. Sadeghi, and J. Seo, "ZnO nanostructures in active antibacterial food packaging: preparation methods, antimicrobial mechanisms, safety issues, future prospects, and challenges," *Food Reviews International,* vol. 38, no. 4, pp. 537-565, 2022.

[12] O. Smirnov, V. Dzhagan, M. Kovalenko, O. Gudymenko, V. Dzhagan, N. Mazur, O. Isaieva, Z. Maksimenko, S. Kondratenko, and M. Skoryk, "ZnO and Ag NP-decorated ZnO nanoflowers: green synthesis using Ganoderma lucidum aqueous extract and characterization," *RSC advances,* vol. 13, no. 1, pp. 756-763, 2023.

[13] D. Vu, "Effects of extraction solvents on phytochemicals and bioactivities of Ganoderma lucidum," *Egyptian Journal of Chemistry,* vol. 66, no. 9, pp. 581-588, 2023.

[14] O. Smirnov, V. Dzhagan, M. Kovalenko, O. Gudymenko, V. Dzhagan, N. Mazur, O. Isaieva, Z. Maksimenko, S. Kondratenko, M. Skoryk, and V. Yukhymchuk, "ZnO and Ag NP-decorated ZnO nanoflowers: green synthesis using Ganoderma lucidum aqueous extract and characterization," *RSC advances,* vol. 13, no. 1, pp. 756-763, 2022.

[15] A. M. Ibrahim, L. M. Mohamed, A. D. H. Aweis, S. Q. Fidow, F. A. Mohamed, S. M. Osman, F. A. Mohamed, I. A. Mohamud, N. M. Roble, and M. M. Osman, "A five-year retrospective analysis of antimicrobial resistance patterns in clinical bacterial isolates from the Jazeera University Laboratory in Mogadishu, Somalia," *BMC Microbiology,* vol. 25, no. 1, p. 779, 2025.

[16] R. A. Jasim, "Evaluation of the antimicrobial activity of Agaricus bisporus mushroom extracts against some human pathogenic bacteria " Master thesis, Department of Biology, College of Science, University of Baghdad, 2020.

[17] E. A. AL-Sudani and S. A. Alash, "Prevalence of Urinary Tract Infections in Adult and Child Patients," *Indian Journal of Public Health,* vol. 10, no. 11, p. 1861, 2019.

[18] Z. A. S. Ali and A. M. Y. Al-Araji, "Evaluation of Copper Nanoparticle Synthesis by Fusarium oxysporum Antibacterial Activity Against Staphylococcus aureus," in *IOP Conference Series: Earth and Environmental Science*, 2024.

[19] A. Can and K. Kizilbey, "Green Synthesis of ZnO Nanoparticles via Ganoderma Lucidum Extract: Structural and Functional Analysis in Polymer Composites," *Gels,* vol. 10, no. 9, p. 576, 2024.

[20] M. A. Alden and L. Yaaqoob, "Evaluation of the Biological Effect Synthesized Zinc Oxide Nanoparticles on Pseudomonas aeruginosa," *Iraqi Journal of Agricultural Sciences,* vol. 53, no. 1, pp. 27-37, 2022.

[21] D. Ranjith Santhosh Kumar, N. Elango, G. D. Selvaraju, P. A. Matthew, S. Palanisamy, H. Cho, F. S. Al Khattaf, A. A. Hatamleh, and A. D. Roy, "Mycosynthesis of zinc oxide nanoparticles coated with silver using Ganoderma lucidum (Curtis) P. Karst and its evaluation of in vitro antidiabetic and anticancer potential," *Journal of Nanomaterials,* vol. 2022, no. 1, p. 2798532, 2022.

[22] A. K. Mandal, S. Katuwal, F. Tettey, A. Gupta, S. Bhattarai, S. Jaisi, D. P. Bhandari, A. K. Shah, N. Bhattarai, and N. Parajuli, "Current Research on Zinc Oxide Nanoparticles: Synthesis, Characterization, and Biomedical Applications," *Nanomaterials (Basel),* vol. 12, no. 17, p. 3066, 2022.

[23] A. Jayachandran, R. A. T, and A. S. Nair, "Green synthesis and characterization of zinc oxide nanoparticles using Cayratia pedata leaf extract," *Biochemesitry and Biophysics Reports,* vol. 26, p. 100995, 2021.

[24] L. Yaaqoob, "Evaluation of the biological effect synthesized iron oxide nanoparticles on Enterococcus faecalis," *Iraqi Journal of Agricultural Sciences,* vol. 53, no. 2, pp. 440-452, 2022.

[25] M. H. Nawar, L. A. Yaaqoob, M. W. Hatem, and A. K. Mohammed, "The effect of nanoparticles preparation from extract of Dodonaea Viscosa L. leaves on the biological performance of the Great Waxworm," in *AIP Conference Proceedings*, 2024.

[26] J. A. A. Abdullah, M. Jimenez-Rosado, A. Guerrero, and A. Romero, "Biopolymer-Based Films Reinforced with Green Synthesized Zinc Oxide Nanoparticles," *Polymers (Basel),* vol. 14, no. 23, p. 5202, 2022.

[27] J. Xu, Y. Huang, S. Zhu, N. Abbes, X. Jing, and L. Zhang, "A review of the green synthesis of ZnO nanoparticles using plant extracts and their prospects for application in antibacterial textiles," *Journal of Engineered Fibers and Fabrics,* vol. 16, p. 15589250211046242, 2021.

[28] W. Ding, X. Zhang, X. Yin, Q. Zhang, Y. Wang, C. Guo, and Y. Chen, "Ganoderma lucidum aqueous extract inducing PHGPx to inhibite membrane lipid hydroperoxides and regulate oxidative stress based on single-cell animal transcriptome," (in eng), *Scientific reports,* vol. 12, no. 1, p. 3139, 2022.

[29] M. Constantin, I. Răut, R. Suica-Bunghez, C. Firinca, N. Radu, A.-M. Gurban, S. Preda, E. Alexandrescu, M. Doni, and L. Jecu, "Ganoderma lucidum-mediated green synthesis of silver nanoparticles with antimicrobial activity," *Materials,* vol. 16, no. 12, p. 4261, 2023.

[30] A. Sanmugam, D. Vikraman, S. Venkatesan, and H. J. Park, "Optical and Structural Properties of Solvent Free Synthesized Starch/Chitosan-ZnO Nanocomposites," *Journal of Nanomaterials,* vol. 2017, no. 1, pp. 1-8, 2017.

[31] H. Agarwal, S. Menon, and V. K. Shanmugam, "Functionalization of zinc oxide nanoparticles using Mucuna pruriens and its antibacterial activity," *Surfaces and Interfaces,* vol. 19, p. 100521, 2020.

[32] S. N. Mazhir, N. K. Abdalameer, L. A. Yaaqoob, and J. K. Hammood, "Cold plasma synthesis of Zinc Selenide Nanoparticles for inhibition bacteria using disc diffusion," *Physics and Chemistry of Solid State,* vol. 23, no. 4, pp. 652-658, 2022.

[33] A. Sirelkhatim, S. Mahmud, A. Seeni, N. H. M. Kaus, L. C. Ann, S. K. M. Bakhori, H. Hasan, and D. Mohamad, "Review on zinc oxide nanoparticles: antibacterial activity and toxicity mechanism," *Nano-micro letters,* vol. 7, pp. 219-242, 2015.

[34] X.-Q. Zhou, Z. Hayat, D.-D. Zhang, M.-Y. Li, S. Hu, Q. Wu, Y.-F. Cao, and Y. Yuan, "Zinc oxide nanoparticles: synthesis, characterization, modification, and applications in food and agriculture," *Processes,* vol. 11, no. 4, p. 1193, 2023.

[35] S. K. Verma, E. Jha, P. K. Panda, J. K. Das, A. Thirumurugan, M. Suar, and S. Parashar, "Molecular aspects of core-shell intrinsic defect induced enhanced antibacterial activity of ZnO nanocrystals," *Nanomedicine (Lond),* vol. 13, no. 1, pp. 43-68, 2018.